Supplementary Figure Legends

Supplementary Figure 1. Imaging characteristics of LOT. Axial contrast-enhanced computed tomography (CT) images of the abdomen (LOT 3) obtained during the corticomedullary phase (A) and excretory phase (B). Multiple heterogeneous intensely enhancing masses during the corticomedullary phase (red arrows) are present. Note large irregular areas of decreased central enhancement during the corticomedullary phase (yellow arrows) which exhibit slow progressive centripetal enhancement during the excretory phase.

Supplementary Figure 2. **Microscopic features of LOT.** (A) Representative H&E images illustrating frequently observed thick walled peritumoral vessels. (B) Small tumorlets in non-neoplastic renal parenchyma in LOT 3 patient. Small subclone (red asterisk) with diverse morphology in one of 16 tumors in LOT 3 (C-D) and LOT 4 (E-F). Subclones are characterized by large intracytoplasmic vacuoles in LOT 3 with germline *TSC1* mutation (D), and more pronounced perinuclear clearing and nuclear membrane irregularities in LOT 4 (F).

Supplementary Figure 3. Somatic mutations from whole exome sequencing (WES) analysis. Oncoplot showing number and types of selected somatic alterations in LOT samples. Frequent non-overlapping mutations were observed in mTOR pathway genes. LOT 6 had *MTOR* gene mutation that is not represented in the oncoplot as WES data from the corresponding normal kidney was not available.

Supplementary Figure 4. Schematic of LOT mutations by next generation sequencing. Sequencing reads with somatic (A) and germline mutations (B) as visualized with Integrated Genome Viewer.

Supplementary Figure 5. Sanger sequencing confirming the mTOR pathway gene mutations. Representative chromatograms of forward and reverse Sanger sequencing from tumor and normal tissue samples.

Supplementary Figure 6. Copy number analysis of chromosome 1 in LOT. Log_2 copy ratio of chromosome 1 and *MTOR* neighborhood on WES in LOTs with *MTOR* mutations. Chromosome copy number in LOT 1, LOT 2 and LOT 5 tumor samples was called by using CNVkit (Version 0.9.5). Figure shows that the three cases consistently have average log2 ratio 0 for chromosome 1, suggesting the presence of two copies of chromosome 1. Mean b-allele frequencies approximate the expected 0.5 value. Lack of divergence from 0.5 indicates no copy neutral loss of heterozygosity. Zoom-in plots of *MTOR* gene neighborhood are also displayed.

Supplementary Figure 7. Somatic mutations and schematic mapping of the mTOR mutations in LOT. (A) Table with somatic mutations in the mTOR protein in 4 LOT from UTSW and 4 tumors (2 from TCGA and 2 from Skala et al[61]) that were morphologically consistent with LOT. (B) Structure context of mTOR mutations as shown in Figure 2A including those from TCGA and Skala et al[61].

Supplementary Figure 1

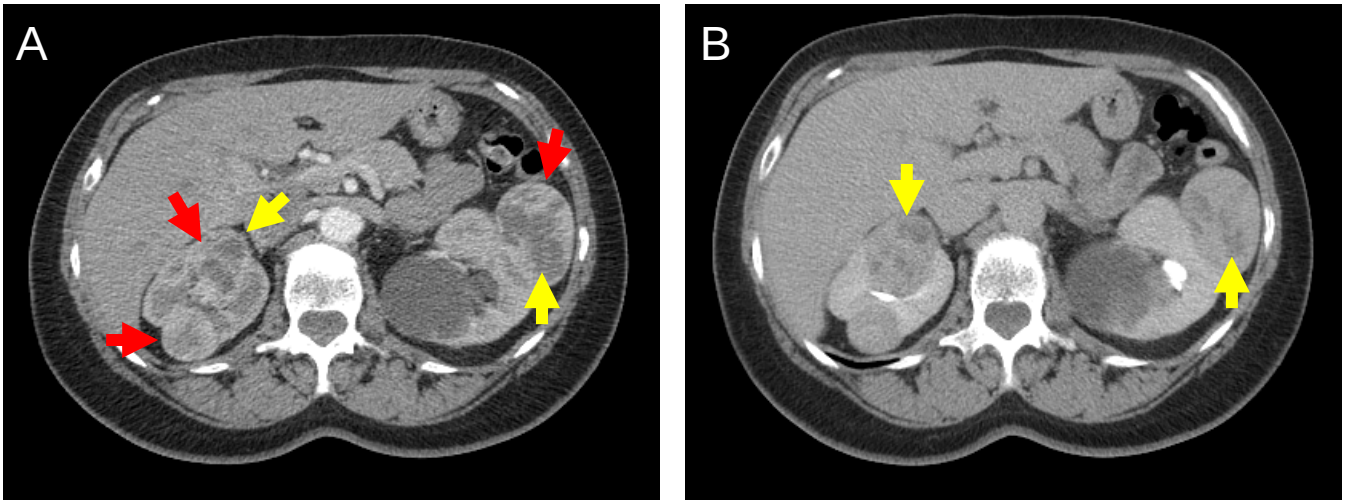

Supplementary Figure 2

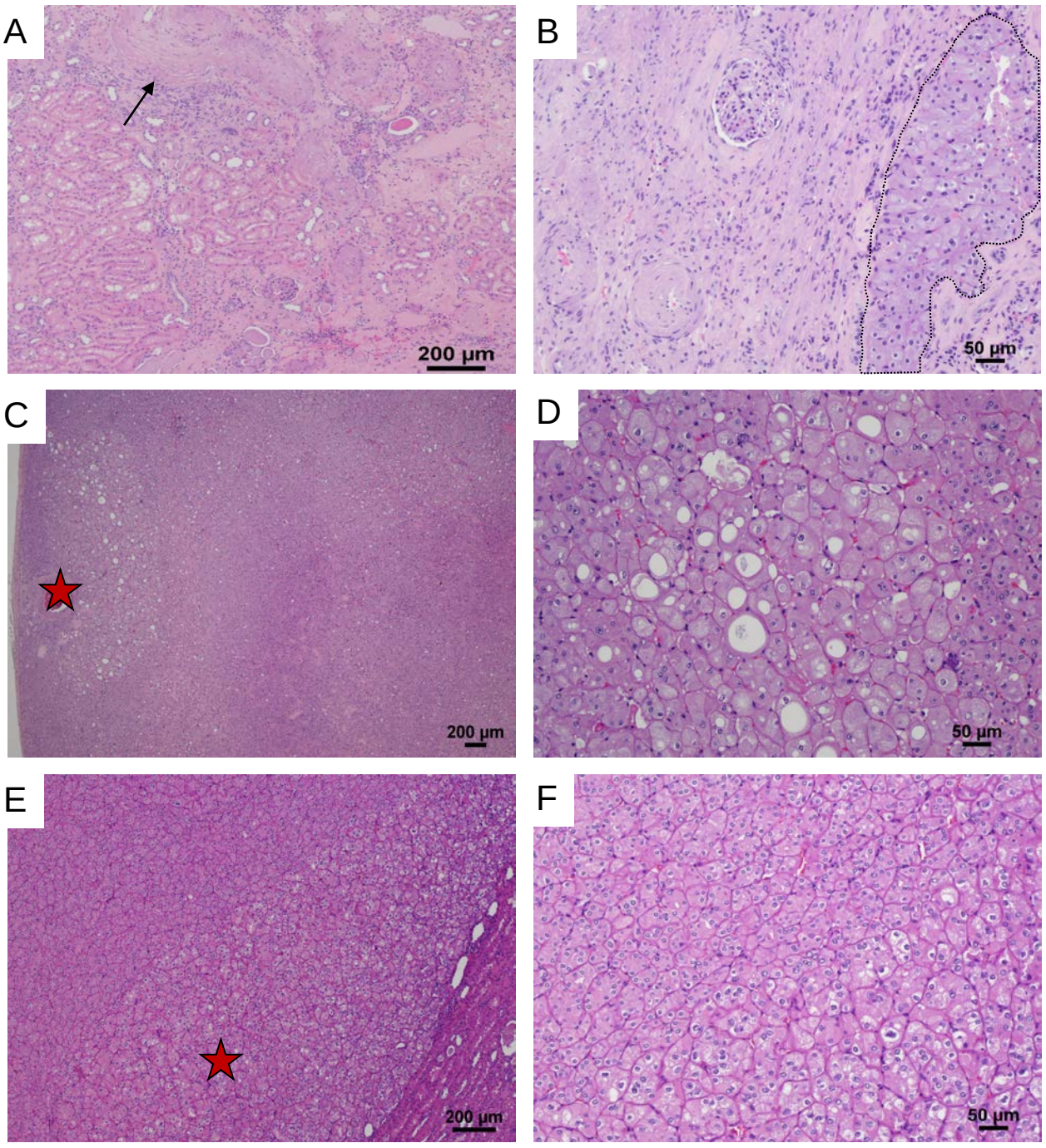

Supplementary Figure 3

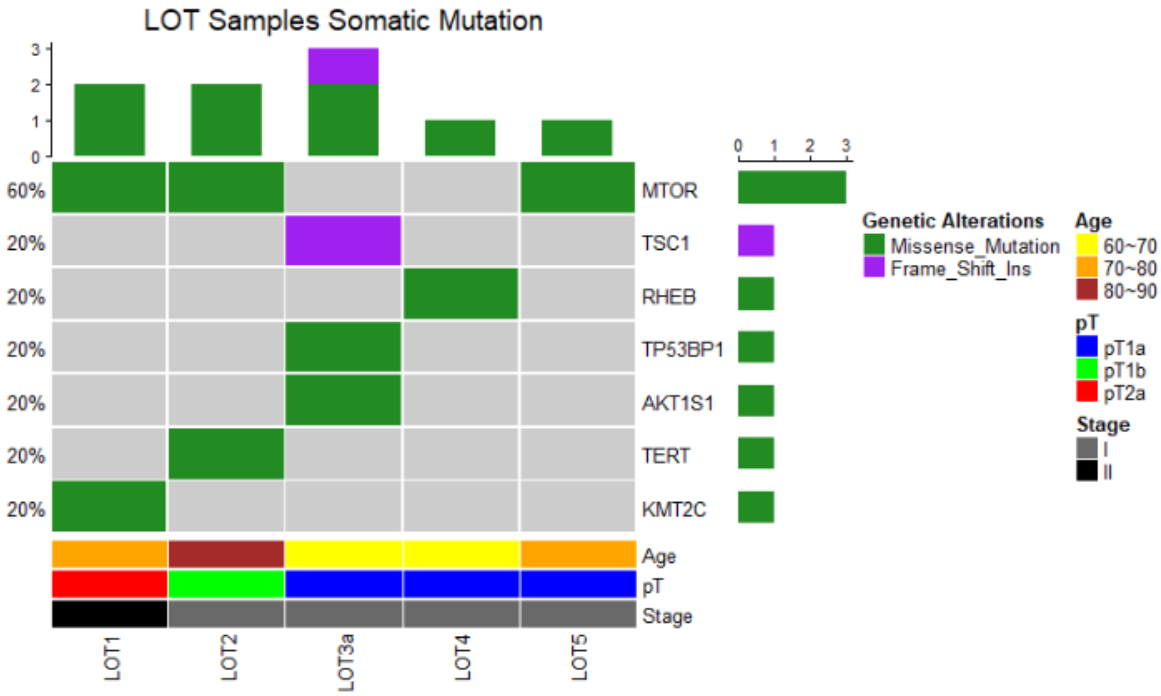

Supplementary Figure 4A

LOT1
NM_004958.3:c.7280T>A

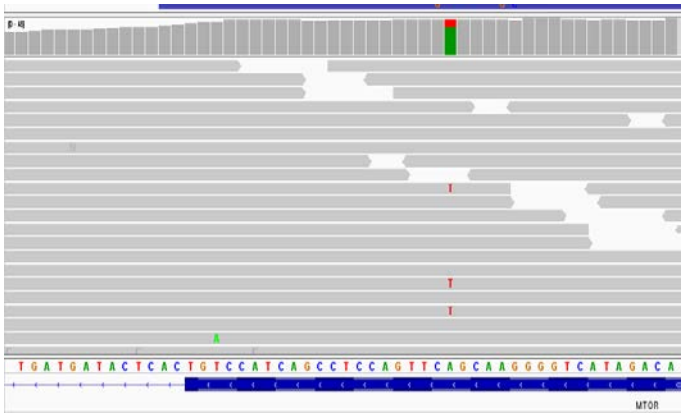

LOT2
NM_004958.3:c.6644C>A

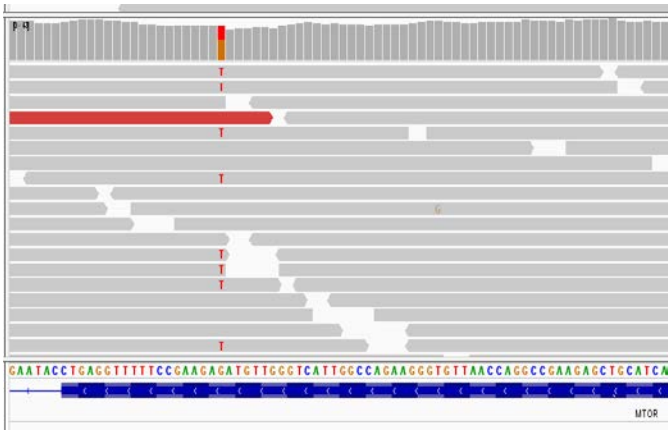

LOT3a
NM_000368.4:c.2273_2276dup

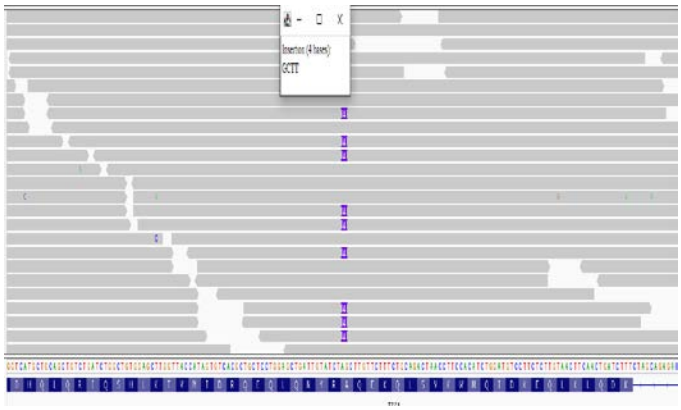

LOT4
NM_005614.3:c.103_104delinsCT

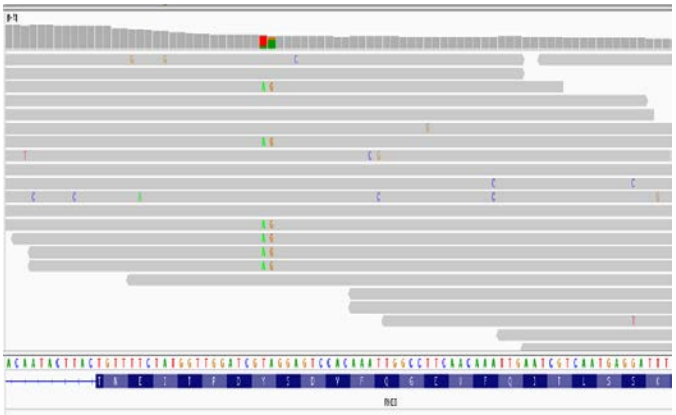

LOT5
NM_004958.3:c.7237_7238delinsCT

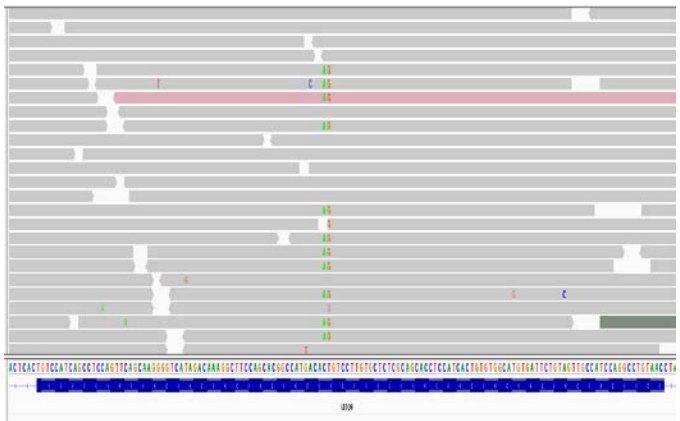

LOT6
NM_004958.3:c.4354_4365del

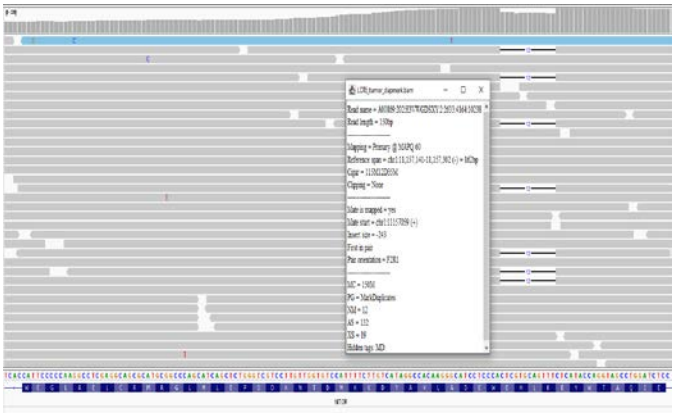

Supplementary Figure 4B

LOT3a
NM_000368.4:c.2208+2T>A

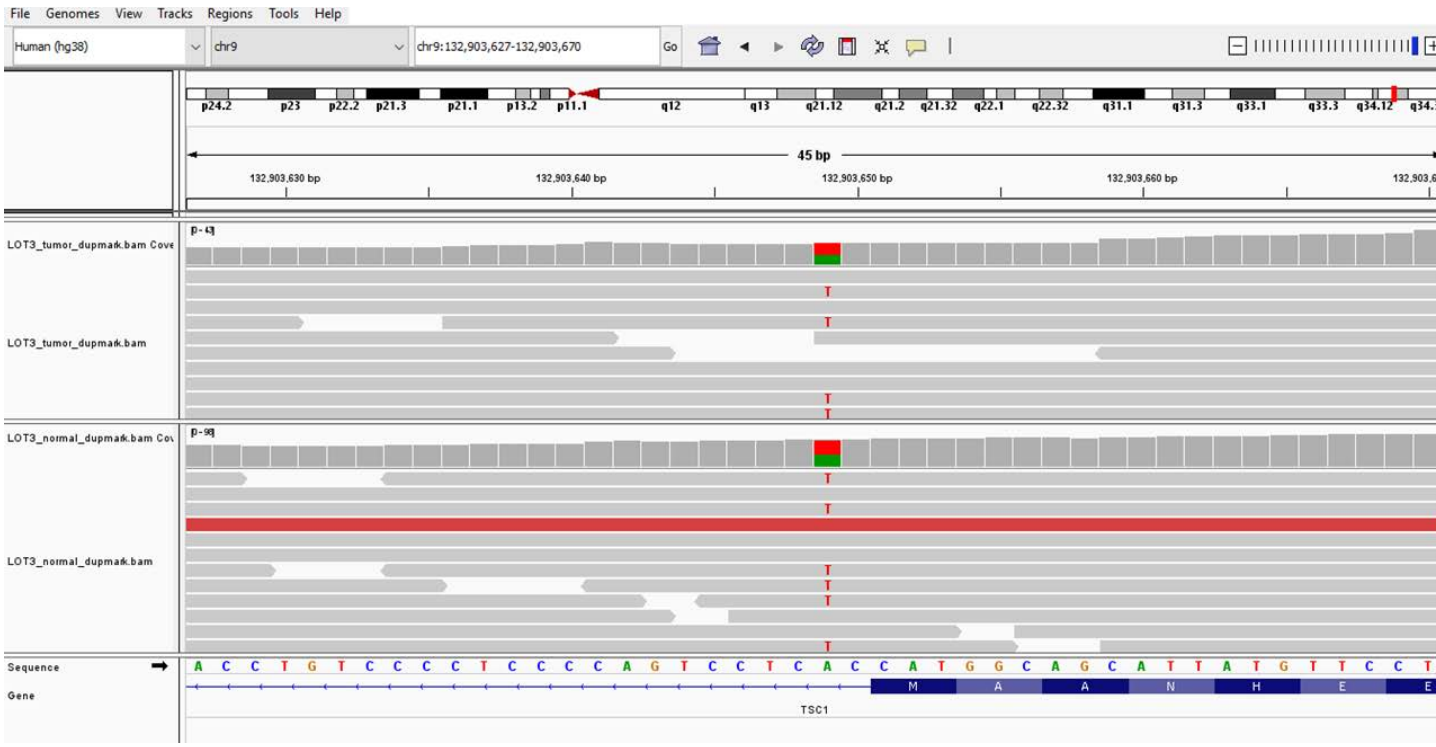

Supplementary Figure 5

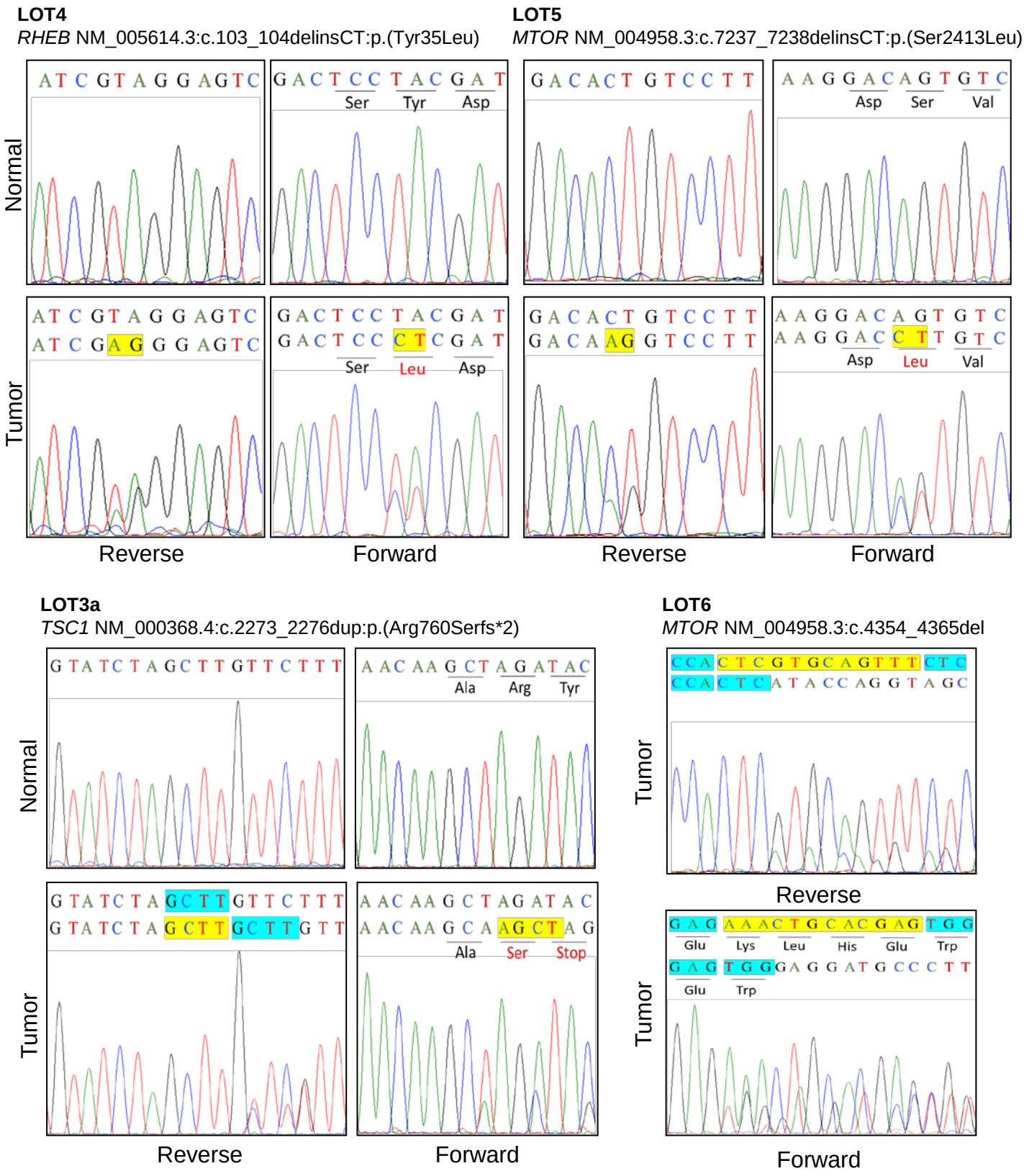

Supplementary Figure 6

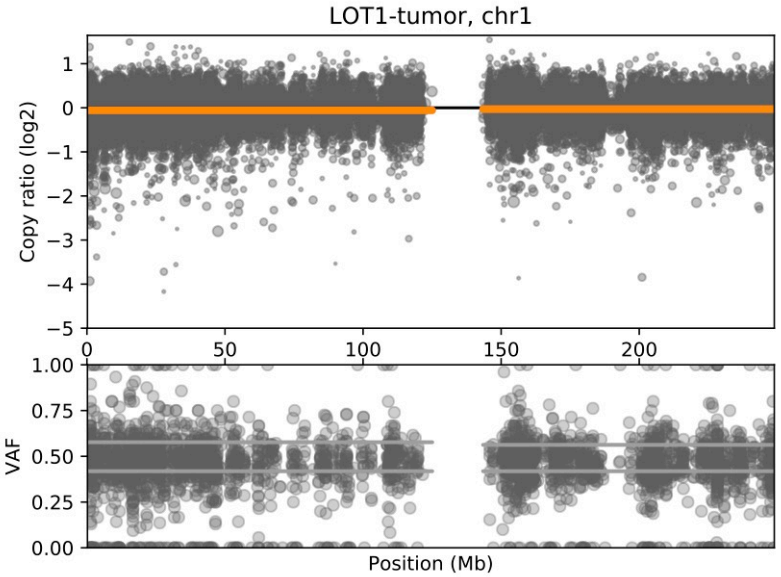

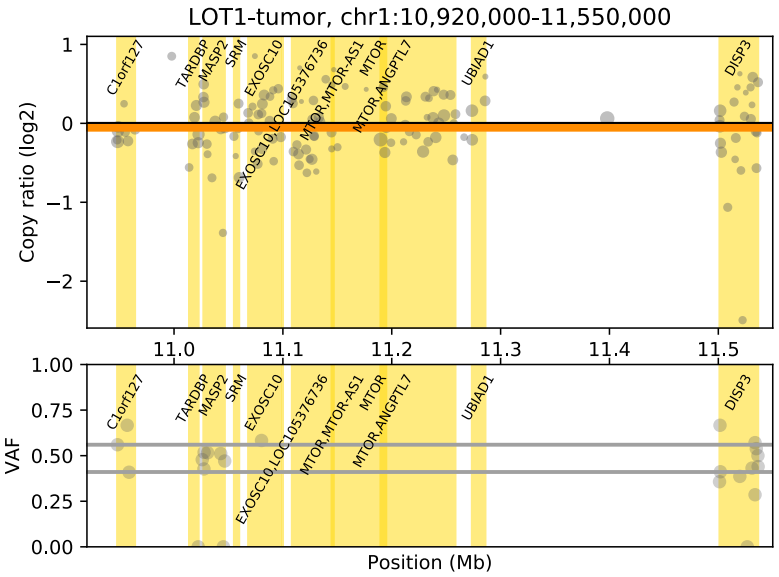

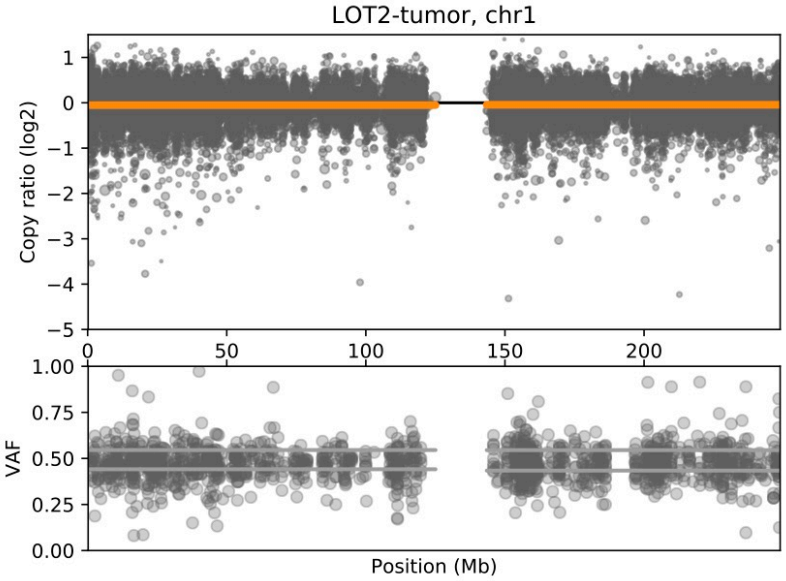

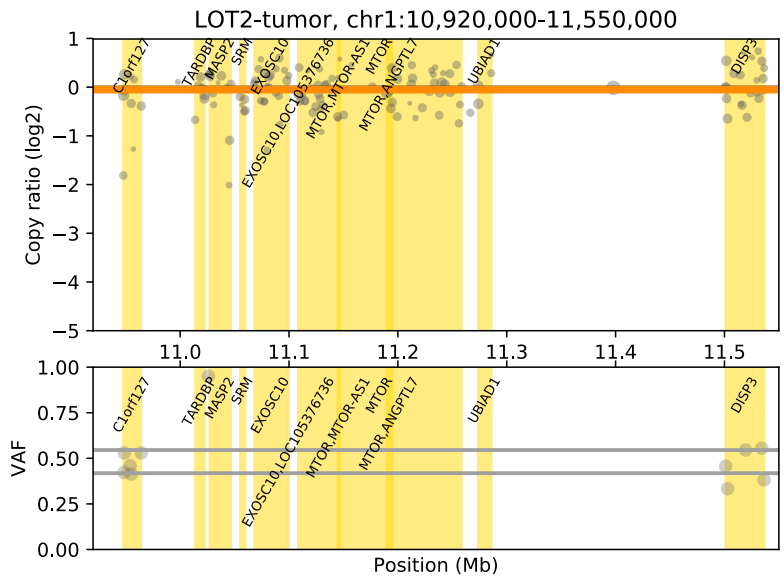

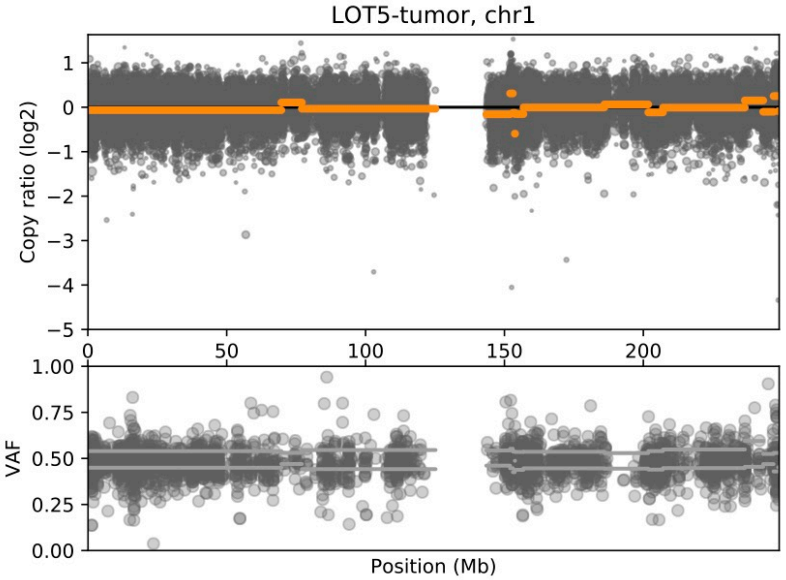

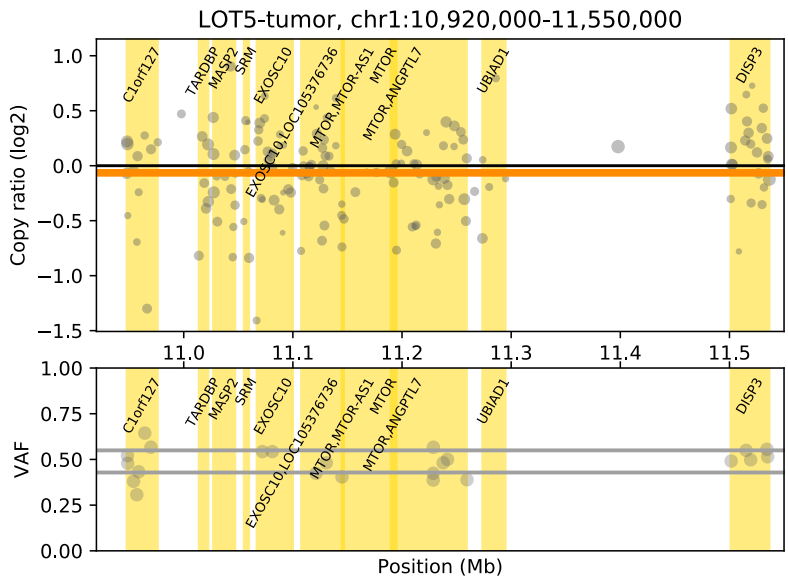

Supplementary Figure 7

A

LOT Sample	Amino Acid Alteration	Variant Classification
LOT1	L2427Q	nonsynonymous SNV
LOT2	S2215Y	nonsynonymous SNV
LOT5	S2413L	nonsynonymous SNV
LOT6	K1452_E1455del	nonframeshift substitution
TCGA-KM-8441 ★	I2017T	nonsynonymous SNV
TCGA-KN-8437 ★	L2427R	nonsynonymous SNV
Skala et al #1	S2215Y	nonsynonymous SNV
Skala et al #2	L2427Q	nonsynonymous SNV

B